# Insertion Reaction of Phenyl Isocyanate into the Ln−C σ-Bond of Organolanthanide Complexes: Synthesis, Characterization, and Crystal Structures of $\{(C_5H_4CH_3)_2Ln[\mu\text{-}\eta^1\text{:}\eta^3\text{-}OC(R)NPh]\}_2$ (Ln = Sm, Dy, Er, Ho; R = *n*-butyl, α-naphthyl)

Xi-geng Zhou,* Li-bei Zhang, Ming Zhu, Rui-fang Cai, and Lin-hong Weng

*Department of Chemistry, Fudan University, Shanghai 200433, People's Republic of China, and State Key Laboratory of Organometallic Chemistry, Chinese Academy of Sciences, Shanghai 200032, People's Republic of China*

Zi-xiang Huang and Qiang-jin Wu

*State Key Laboratory of Structural Chemistry, Fuzhou 350002, People's Republic of China*

*Received April 30, 2001*



$Cp'_2LnR(THF)$ ($Cp' = C_5H_4CH_3$) reacted with phenyl isocyanate to form the PhNCO insertion products $[Cp'_2Ln(OC(R)NPh)]_2$ [R = *n*-butyl, Ln = Sm (**1**), Dy (**2**), Er (**3**); R = α-naphthyl, Ln = Dy (**4**)]. It was found that an excess of PhNCO did not affect the nature of the final complexes, a single insertion only being observed and excess PhNCO forming a cyclotrimer (**5**). The reaction of $Cp'HoCl_2(THF)_3$ with $Bu^nLi$ and subsequently with 2 equiv of PhNCO in THF gave $Ho[OC(Bu^n)NPh)]_3$ (**6**) and $[Cp'_2Ho(OC(Bu^n)NPh)]_2$ (**7**), which can be rationalized by the rearrangement reaction of the di-insertion product $Cp'Ho[OC(Bu^n)NPh]_2(THF)_x$. The structures of **1**, **4**·THF, **5**·THF and **7** were determined by X-ray diffraction, revealing an unusual bonding mode of the amido groups arising from the insertion of PhNCO into the Ln−C σ-bonds and that the O···C···N fragment of the OC(R)NPh ligand acts as both a bridging and side-on chelating group.

## Introduction

Organolanthanide alkyl (aryl) complexes continue to attract considerable attention by virtue of the diverse reactivities arising from the Ln−C σ-bond. These species have been utilized as catalysts in a number of transformations involving alkenes and imine and in stoichiometric reactions with organic functionality groups.[1] In sharp contrast to the extensive chemistry of bis(cyclopentadienyl)lanthanide alkyl (aryl) complexes, very little is known about the behavior of monocyclopentadienyllanthanide dialkyls (or diaryls) due to ligand redistribution in solution.[2] On the other hand, although organolanthanide alkyls and aryls are important intermediates in homogeneous catalysis and organometallic synthesis,[3] little attention has focused on lanthanide *n*-butyl derivatives due to the likelihood of β-hydrogen elimination and therefore instability which leads to difficulty in studying further reactivity.[4]

Insertions of isocyanates into main group metal−carbon and transition metal−carbon bonds have been extensively studied. The accumulated information in this field indicates that the occurrence of the insertion strongly depends on the degree of steric saturation around the central metal ion and the nature of the alkyl ligands.[5] However, there is essentially nothing known about isocyanate insertion into Ln−C σ bonds.[6,7] To better understand the reactivity of organolanthanide complexes toward isocyanates, in this paper we report the synthesis, characterization, and crystal structures of the insertion products obtained from the reaction of phenyl isocyanate with organolanthanide alkyl (aryl) complexes.

## Results and Discussion

**Synthesis and Characterization of PhNCO Insertion Products $[Cp'_2LnOC(Bu^n)NPh]_2$ (Ln = Sm, Dy, Er).** The reaction of $Cp'_2LnCl$ with $Bu^nLi$ and

(1) (a) Arredondo, V. M.; Tian, S.; McDonald, F. E.; Marks, T. J. *J. Am. Chem. Soc.* **1999**, *121*, 3633. (b) Molander, G. A.; Retsch, W. H. *J. Am. Chem. Soc.* **1997**, *119*, 8817.

(2) Cotton, S. A. *Coord. Chem. Rev.* **1997**, *160*, 93.

(3) (a) Heeres, H. J.; Meetsma, A.; Teuben, J. H. *Organometallics* **1990**, *9*, 1508. (b) Evans, W. J.; Wayda, A. L.; Hunter, W. E.; Atwood, J. L. *J. Chem. Soc., Chem. Commun.* **1981**, 706. (c) Jeske, G.; Lauke, H.; Mauermann, H.; Swepston, P. N.; Schumann, H.; Marks, T. J. *J. Am. Chem. Soc.* **1985**, *107*, 8091.

(4) (a) Schumann, H.; Genthe, W.; Bruncks, N. *Angew. Chem., Int. Ed. Engl.* **1981**, *20*, 119. (b) Watson, P. L.; Roe, D. C. *J. Am. Chem. Soc.* **1982**, 104, 6471. (c) Evans, W. J.; Wayda, A. L.; Hunter, W. E.; Atwood, J. L. *J. Chem. Soc., Chem. Commun.* **1981**, 292.

(5) (a) Braunstein, P.; Nobel, D. *Chem. Rev.* **1989**, *89*, 1927. (b) Koschmieder, S. U.; Wilkinson, G.; Hussain-Bates, B.; Hursthouse, M. B. *J. Chem. Soc., Dalton Trans.* **1992**, 19. (c) Forster, G. D.; Hogarth, G. *J. Chem. Soc., Dalton Trans.* **1993**, 2539. (d) Legzdins, P.; Phillips, E. C.; Rettig, S. J.; Trotter, J.; Veltheer, J. E.; Yee, V. C. *Organometallics* **1992**, *11*, 3104. (e) Paul, F.; Fischer, J.; Ochsenbein, P.; Osborn, J. A. *Angew. Chem., Int. Ed. Engl.* **1993**, *32*, 1638.

(6) Evans, W. J.; Forrestal, K. J.; Ziller, J. W. *J. Am. Chem. Soc.* **1998**, *120*, 9273.

(7) Evans, W. J.; Randy N. R.; Joseph, B.-D.; Ziller, J. W. *J. Organomet. Chem.* **1998**, *569*, 89.

10.1021/om010346y CCC: $20.00 
Publication on Web 11/29/2001

**Scheme 1**

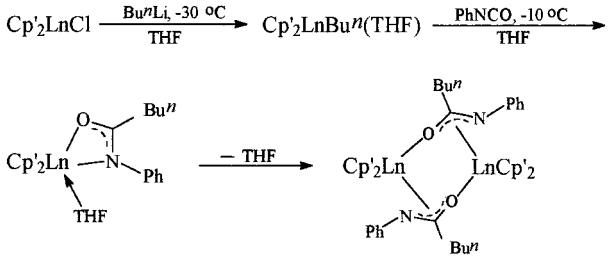


Cp' = $C_5H_4CH_3$; Ln = Sm (**1**), Dy (**2**); Er (**3**)

subsequently with phenyl isocyanate provided the dinuclear products $[Cp'_2LnOC(Bu^n)NPh]_2$ [Ln = Sm (**1**), Dy (**2**), Er (**3**)]. The formation of complexes **1**−**3** was interpreted as an isocyanate molecule insertion into the Ln−C $\sigma$-bond of the intermediate $Cp'_2LnBu^n(THF)$,[4a] as shown in Scheme 1. It is noteworthy that for ytterbium with the stronger reducibility, its analogue could not be obtained in a similar manner. The reaction of $Cp'_2$-YbCl with $Bu^n$Li, followed with PhNCO in THF, led to a complex product mixture under the same conditions, since $Cp'_2$YbCl can be partially reduced to divalent $Cp'_2$-Yb by $Bu^n$Li as observed in $(C_5H_5)_2$YbCl.[4c] In addition, no insertion of the Cp′−Ln bonds was observed at ambient temperature in excess amount of PhNCO even with a longer reaction time.

All the compounds were characterized by elemental analyses and IR and MS spectral data, which were in good agreement with the proposed structures. Complexes **1**−**3** are moderately sensitive toward moisture and air. They are soluble in THF, but less soluble in *n*-hexane. In the mass spectra, all the compounds are characterized by the loss of the Cp′ group from the molecular ion with the $[M - Cp']^+$ ion as a strong peak. In the IR spectral data of **1**−**3**, the band is observed at ca. 1570 $cm^{-1}$, which may be assigned to the absorption of the delocalized mode of the −O···C···N− unit of the resulting amido ligand.[8] The bonding mode was proven by X-ray single-crystal diffraction on complex **1**.

The crystal structure of complex **1** (Figure 1) reveals a centrosymmetric dimer. Selected bond distances and angles are compiled in Table 1. X-ray analysis shows an unusual bonding mode of the $OC(Bu^n)NPh$ ligand and that the O···C···N fragment of the amido ligand acts as both a bridging and side-on chelating group. Each samarium atom is coordinated by two $\eta^5$-$C_5H_4CH_3$ groups, one chelating $\eta^3$-$OC(Bu^n)NPh$ ligand, and one bridging oxygen atom from another $OC(Bu^n)NPh$ ligand. Both the O(1)−C(13) and the N(1)−C(13) distances of 1.305(5) and 1.296(5) Å lie between single- and double-bond distances.[9,10] This suggests some electronic delocalization over the O−C−N unit. Consistent with this, the Sm(1)−N(1A) distance of 2.515(3) Å is slightly shorter than the Sm←:N donor bond,[6,11] and there is a weak interaction between Sm(1A) and C(13).[12] The

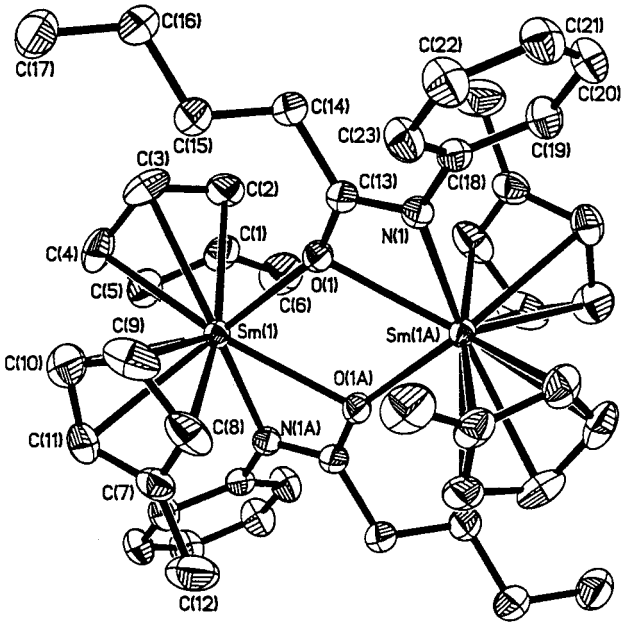


**Figure 1.** ORTEP diagram of $[Cp'_2SmOC(Bu^n)NPh]_2$ (**1**) with the probability ellipsoids drawn at the 30% level.

**Table 1. Selected Bond Lengths (Å) and Angles (deg) in 1**[a]

| Bond Distances | | | |
|---|---|---|---|
| Sm(1)−O(1) | 2.374(3) | Sm(1)−N(1A) | 2.515(3) |
| Sm(1)−O(1A) | 2.529(3) | Sm(1A)−C(13) | 2.938(4) |
| Sm(1)−C(3) | 2.710(5) | Sm(1)−C(10) | 2.713(5) |
| Sm(1)−C(4) | 2.713(5) | Sm(1)−C(9) | 2.725(5) |
| Sm(1)−C(5) | 2.738(5) | Sm(1)−C(11) | 2.747(5) |
| Sm(1)−C(2) | 2.747(5) | Sm(1)−C(8) | 2.759(5) |
| Sm(1)−C(1) | 2.769(5) | Sm(1)−C(7) | 2.772(5) |
| O(1)−C(13) | 1.305(5) | N(1)−C(13) | 1.296(5) |
| N(1)−C(18) | 1.413(5) | C(13)−C(14) | 1.513(6) |

| Bond Angles | | | |
|---|---|---|---|
| O(1)−Sm(1)−N(1A) | 119.8(1) | O(1)−Sm(1)−O(1A) | 69.8(1) |
| N(1A)−Sm(1)−O(1A) | 51.9(1) | Sm(1)−O(1)−Sm(1A) | 110.2(1) |
| C(13)−O(1)−Sm(1) | 153.8(3) | C(13)−O(1)−Sm(1A) | 94.7(2) |
| O(1)−C(13)−N(1) | 116.1(4) | C(13)−N(1)−C(18) | 123.5(3) |
| N(1)−C(13)−C(14) | 124.8(4) | O(1)−C(13)−C(14) | 118.6(4) |

[a] Symmetry transformation (A): $-x$, $2-y$, $2-z$.

delocalization is also verified by the fact that the Sm(1)−O(1A) distance of 2.529(3) Å is similar to the Sm(1)−N(1A) distance of 2.515(3) Å. The distances of C(13)−C(14) and N(1)−C(18) correspond well to single bonds. The bond angles around C(13) are consistent with $sp^2$ hybridization.

Significantly, it is different from the results observed in $[Cp_2Ln(\mu\text{-}OR)]_2$-type organolanthanide complexes, where two bridging Ln−O distances are usually similar,[13,19,23] that the Sm(1)−O(1) distance of 2.374(3) Å in



(8) Wilkins, J. D. *J. Organomet. Chem*. **1974**, *67*, 269.
(9) Allen, F. H.; Kennard, O.; Watson, D. G.; Brammer, L.; Orpen, A. G. *J. Chem. Soc., Perkin Trans*. **1987**, S1.
(10) Wu, Z. Z.; Zhou, X. G.; Zhang, W.; Xu, Z.; You, X. Z.; Huang, X. Y. *J. Chem. Soc., Chem. Commun*. **1994**, 813.
(11) Obora, Y.; Ohta, T.; Stern, C. L.; Marks, T. J. *J. Am. Chem. Soc*. **1997**, *119*, 3745.
(12) Zhou, X. G.; Zhang, L. B.; Huang, Z. E.; Cai R. F.; Huang, X. Y. *Chin. J. Struct. Chem*. **1999**, *18*, 373.
(13) (a) Steudel, A.; Stehr, J.; Siebel, E.; Fischer, R. D. *J. Organomet. Chem*. **1998**, *570*, 89. (b) Evans, W. J.; Sollberger, M. S.; Shreeve, J. L.; Olofson, J. M.; Hain, J. H.; Ziller, J. W. *Inorg. Chem*. **1992**, *31*, 2492. (c) Evans, W. J.; Dominguez, R. D.; Hanusa, T. P. *Organometallics* **1986**, *5*, 1291. (d) Schumann, H.; Palamidis, E.; Loebel, J. *J. Organomet. Chem*. **1990**, *384*, C49. (e) Zhou, X. G.; Ma, W. W.; Huang, Z. E.; Cai, R. F.; You, X. Z.; Huang, X. Y. *J. Organomet. Chem*. **1997**, *545*−*546*, 309. (f) Zhou, X. G.; Ma, H. Z.; Huang, X. Y.; You, X. Z. *J. Chem. Soc., Chem. Commun*. **1995**, 2483. (g) Stults, S. D.; Anderson, R. A.; Zalkin, A. *Organometallics* **1990**, *9*, 623.
(14) (a) Wu, Z. Z.; Xu, Z.; You, X. Z.; Zhou, X. G.; Huang, X. Y.; Chen, J. T. *Polyhedron* **1994**, *13*, 379. (b) Evans, W. J.; Ulibarri, T. A.; Chamberlain, L. R. Ziller, J. W. *Organometallics* **1990**, *9*, 2124. (c) Evans, W. J.; Grate, J. W.; Bloom, I.; Hunter, W. E.; Atwood, J. L. *J. Am. Chem. Soc*. **1985**, *107*, 405. (d) Evans, W. J.; Foster, S. E. *J. Organomet. Chem*. **1992**, *433*, 79.

**1** is significantly shorter than the Sm(1)−O(1A) distance of 2.529(3) Å. The latter is within the 2.44(2)−2.64(2) Å range of the Sm←:$OR_2$ bond for neutral oxygen donor ligands.[14] The Sm−O−Sm angle of 110.2(1)° is slightly larger than those observed in other oxygen-bridging complexes, 104.3(2)−108.3(1)°, but the O−Sm−O angle of 69.8(1)° is smaller than the corresponding values, 71.7(1)−75.7(2)°.[13,19,23] These may be attributed to the steric effect caused by the side-on chelating coordination of $Sm^{3+}$ to the O···C···N fragment of the amido group. It is noteworthy that when the differences in the ionic radii are considered,[15] the chelating Sm−O and Sm−N distances are compatible with the corresponding values in $Cp_2ZrMe[OC(Me)NPh]$, 2.298(4) and 2.297(4) Å.[16]

The average Sm−C($\eta^5$-Cp′) distance of 2.736(5) Å is similar to those found in other trivalent samarium complexes, such as $[(C_5H_4Me)_2(THF)Sm(\mu\text{-}Cl)]_2$, 2.72(3) Å;[17] $Cp_3Sm(THF)$, 2.75(2) Å;[14a] and $(OCH_2CH_2CH_2CH\text{-}CH_2C_5H_4)_2SmCl$, 2.721(7) Å.[18] The Sm(1A)−C(13) distance of 2.938(4) Å is longer than the average Sm−C($\eta^5$-Cp′) distance, indicating a weak interaction between Sm(1A) and C(13).[12]

**Synthesis and Characterization of $[Cp'_2Dy(OC(Np)NPh)]_2$ (4).** To understand the factors affecting the insertion of isocyanate into the lanthanide−carbon bond, the reaction of isocyanate with rare earth aryl complex $Cp'_2DyNp$ (Np = α-naphthyl) was also studied, which provided the corresponding insertion product $[Cp'_2Dy(OC(Np)NPh)]_2$, indicating the occurrence of the insertion is less affected by the properties of the alkyl ligands. In addition, it was found that a large excess of PhNCO did not affect the nature of the final compound, a single insertion only being observed.

Complex **4** is moderately sensitive toward moisture and air. It is soluble in THF, but less soluble in *n*-hexane. Figure 2 shows the molecular structure of **4**. Selected bond distances and angles are listed in Table 2. Each dysprosium atom carries two $\eta^5$-methylcyclopentadienyl groups and is chelated by one of the amido ligands, the oxygen atom of which then bridges over to another Dy atom. The Dy−C(Cp′) distances range from 2.59(4) to 2.77(3) Å and average 2.67(4) Å. The average value is similar to those found in other $Cp_2Dy$-containing compounds, such as $[Cp_2Dy(OCMe{=}CHCH_3)]_2$, 2.67(1) Å.[19] The chelating Dy−O distance of 2.481(13) Å is larger than the bridging Dy−O distance of 2.357(13) Å. The Dy−N(1), Dy−O(1), and Dy−C(13) distances of 2.483(14), 2.481(13), and 2.916(15) Å are slightly longer than the corresponding distances in **1**, respectively, when the differences in the ionic radii are considered.[15] This shows that the tendency toward a $\eta^3$-fashion coordination for the OC(R)NPh group is to decrease when the steric crowding increases.

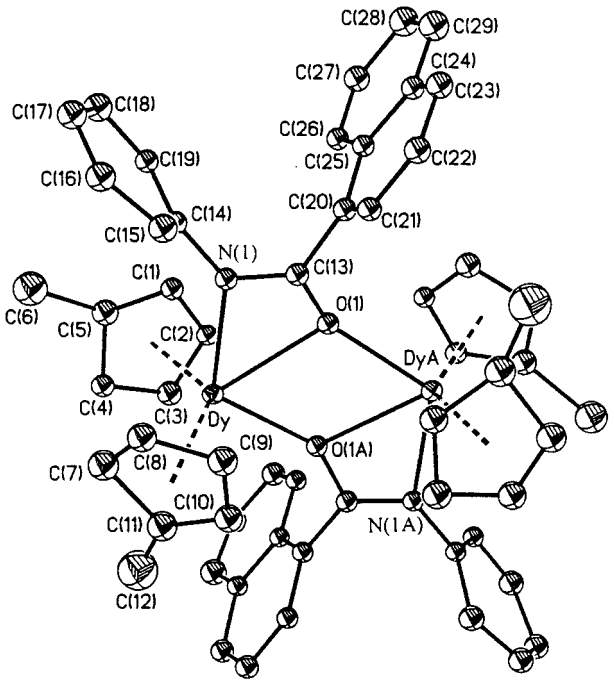


**Figure 2.** ORTEP diagram of $[Cp'_2DyOC(Np)NPh]_2$ (**4**) with the probability ellipsoids drawn at the 30% level.

**Table 2. Selected Bond Lengths (Å) and Angles (deg) in 4[a]**

| Bond Distances | | | |
|---|---|---|---|
| Dy−O(1A) | 2.357(13) | Dy−N(1) | 2.483(15) |
| Dy−O(1) | 2.481(13) | Dy−C(13) | 2.916(4) |
| Dy−C(11) | 2.59(4) | Dy−C(10) | 2.61(3) |
| Dy−C(2) | 2.67(3) | Dy−C(1) | 2.67(3) |
| Dy−C(3) | 2.67(3) | Dy−C(7) | 2.67(4) |
| Dy−C(9) | 2.68(4) | Dy−C(4) | 2.71(3) |
| Dy−C(8) | 2.71(3) | Dy−C(5) | 2.77(3) |
| O(1)−C(13) | 1.30 (2) | N(1)−C(13) | 1.25(2) |
| N(1)−C(18) | 1.46(2) | C(13)−C(20) | 1.49(3) |
| **Bond Angles** | | | |
| O(1A)−Dy−N(1) | 119.4(5) | O(1)−Dy−O(1A) | 67.9(5) |
| N(1)−Dy−O(1) | 51.5(5) | Dy−O(1)−Dy(A) | 111.0(5) |
| C(13)−O(1)−Dy | 95.8(13) | C(13)−O(1)−Dy(A) | 148.6(15) |
| O(1)−C(13)−N(1) | 115.1(19) | C(13)−N(1)−C(14) | 124.5(18) |
| N(1)−C(13)−C(20) | 124.8(18) | O(1)−C(13)−C(20) | 119.5(19) |

[a] Symmetry transformation (A): $1-x, -y, z$.

**Cyclopolymerization of Phenyl Isocyanate Catalyzed by Complex 2.** In contrast to the reaction of $(C_5Me_5)_3Sm$, where a second equivalent of phenyl isocyanate can be incorporated into the first insertion product to form $(C_5Me_5)_2Sm[OC(C_5Me_5)N(Ph)C(NPh)O]$,[6] we have found that only observable products are complex **2** and cyclotrimer $(PhNCO)_3$ (**5**) in the reaction of **2** and excess phenyl isocyanate or when $Cp'_2LnBu^n(THF)$ reacted with excess phenyl isocyanate. This might be attributed to the difference of the steric crowding of the center metal in the two cases. For the more sterically saturated $(C_5Me_5)_2Sm[OC(C_5Me_5)N(Ph)C(NPh)O]$ the insertion of the third PhNCO molecule is prevented, so a di-insertion product is isolated, while for the less sterically demanding $Cp'_2Ln(OCNPh)_2Bu^n$ the approach of the third PhNCO to the metal center is less hindered,

(15) Shannon, R. D. *Acta Crystallogr.* **1976**, A32, 751.
(16) Gambarotta, S.; Strologo, S.; Floriani, C.; Chiesi-Villa, A.; Guastini, C. *Inorg. Chem.* **1985**, *24*, 654.
(17) Evans, W. J.; Keyer, R. A.; Ziller, J. W. *J. Organomet. Chem.* **1993**, *450*, 115.
(18) Zhang, L. B.; Zhou, X. G.; Cai, R. F.; Weng, L. H. *J. Organomet. Chem.* **2000**, *612*, 176.
(19) Wu, Z. Z.; Xu, Z.; You, X. Z.; Zhou, X. G.; Huang, X. Y. *J. Organomet. Chem.* **1994**, *483*, 107.
(20) Chisholm, M. H.; Cotton, F. A.; Folting, K.; Huffman, J. C.; Ratermann, A. L.; Shamshoum, E. S. *Inorg. Chem.* **1984**, *23*, 4423.
(21) Lai, R.; Mabille, S.; Croux, A.; Bot, S. L. *Polyhedron* **1991**, *10*, 463.
(22) (a) Wu, Z. Z.; Xu, Z.; You, X. Z.; Wang, H. J.; Zhou, X. G. *Polyhedron* **1993**, *12*, 677. (b) Huang, X. Y.; Zhou, X. G.; Zhang, L. X.; Feng, X. J.; Cai, R. F.; Huang, Z. E. *Chin. J. Struct. Chem.* **1998**, *17*, 449.
(23) Zhou, X. G.; Huang, Z. E.; Cai, R. F.; Zhang, L. B.; Zhang, L. X.; Huang, X. Y. *Organometallics* **1999**, *18*, 4128.

**Table 3. Selected Bond Lengths (Å) and Angles (deg) in 5**

| Bond Distances | | | |
|---|---|---|---|
| C(1)−O(1) | 1.202(2) | C(1)−N(1) | 1.383(2) |
| C(1)−N(3) | 1.389(2) | N(1)−C(2) | 1.390(2) |
| N(1)−C(4) | 1.452(2) | C(2)−O(2) | 1.198(2) |
| C(2)−N(2) | 1.389(2) | N(2)−C(3) | 1.387(2) |
| N(2)−C(10) | 1.453(2) | C(3)−O(3) | 1.198(2) |
| C(3)−N(3) | 1.392(2) | N(3)−C(16) | 1.449(2) |
| **Bond Angles** | | | |
| O(1)−C(1)−N(1) | 122.59(14) | O(1)−C(1)−N(3) | 122.27(14) |
| N(1)−C(1)−N(3) | 115.13(13) | C(1)−N(1)−C(4) | 117.34(12) |
| C(1)−N(1)−C(2) | 124.85(12) | C(2)−N(1)−C(4) | 117.43(12) |
| N(2)−C(2)−N(1) | 115.04(12) | C(3)−N(2)−C(2) | 124.83(12) |
| C(3)−N(2)−C(10) | 118.00(12) | C(2)−N(2)−C(10) | 116.77(12) |
| N(2)−C(3)−N(3) | 114.73(13) | C(1)−N(3)−C(3) | 124.86(13) |
| C(1)−N(3)−C(16) | 117.41(12) | C(3)−N(3)−C(16) | 117.72(12) |

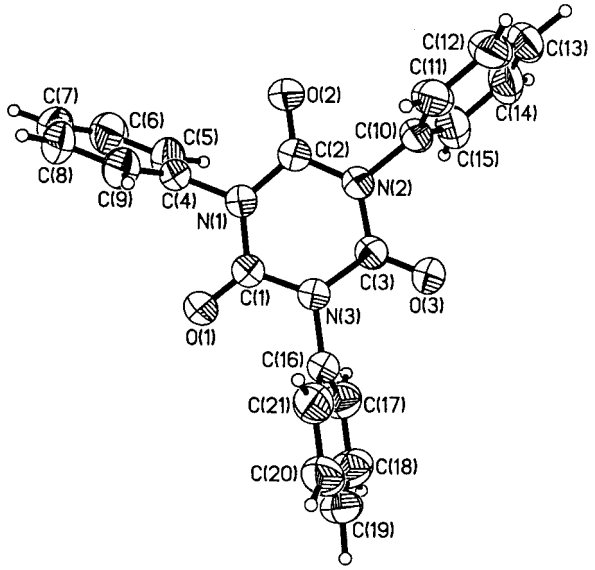


**Figure 3.** ORTEP diagram of $(PhNCO)_3$ (**5**) with the probability ellipsoids drawn at the 30% level.

which should prevent the insertion from staying at the 1:2 adduct and catalyze the excess PhNCO to polymerize cyanurates $(PhNCO)_3$. Reactions of this type have previously been observed in the insertion of isocyanate into the M−O bond.[20] It is noteworthy that the cyclotrimer reaction is readily complicated at room temperature by some side reactions, so the reaction mixture must be slowly warmed to room temperature. The IR spectra of **5** appeared a strong band at 1708 $cm^{-1}$, which might be attributed to a C═O stretch.

The cyclotrimer **5** was proven by the X-ray analysis. Selected bond distances and bond angles are compiled in Table 3. It can be seen (Figure 3) that the molecule structure of **5** confirms closely a six-membered ring constitution, in which the three substrate molecules are joined by the C−N coupling. The average carbon−oxygen distance [1.199(2) Å] agrees well with the corresponding formal C═O distances. The average carbon(ring)−nitrogen distance [1.388(2) Å] is in the middle of the 1.321−1.416 Å range of $C(sp^2)$−N distances.[9] The N(1), C(1), N(2), C(2), N(3) and C(3) atoms are coplanar within experimental error.

**Reaction of Monocyclopentadienyllanthanide Dibutyl with Phenyl Isocyanate.** To gain more insight into the insertion of isocyanate into the Ln−C $\sigma$-bond, the reaction of isocyanate with organolanthanide dialkyls was also studied. It was found that

**Scheme 2**

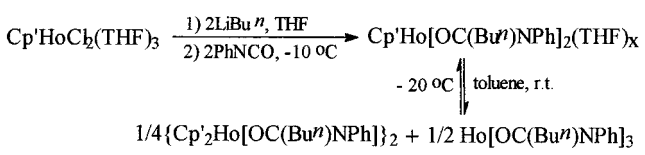


$Cp'Ho(Bu^n)_2(THF)_n$ reacted with 2 equiv of phenyl isocyanate, forming the di-insertion product $Cp'Ho[OC(Bu^n)NPh]_2(THF)_x$ by the route we propose in Scheme 2. However, attempts to isolate the pure product were unsuccessful. $Cp'Ho[OC(Bu^n)NPh]_2(THF)_x$ is susceptible to heat and decomposes easily to $Ho[OC(Bu^n)NPh]_3$ (**6**) and $[Cp'_2Ho(OC(Bu^n)NPh)]_2$ (**7**) in toluene at room temperature. It is noteworthy that the above disproportionation reaction of $Cp'Ln[OC(Bu^n)NPh]_2$ is reversible. The rate of this disproportionation increases considerably at elevated temperature, but when the temperature is below −20 °C, the rearrangement products are slowly transformed into the starting material. Significantly, when an excess of PhNCO is used, a cycloaddition product (**5**) and unidentified polymers of some kinds were observed too.

It will be noted that PhNCO has inserted into all the available Ln−C $\sigma$-bonds, although similar complete insertion of RNCO has been observed in only a few cases.[5b] For example, only one of the M−C $\sigma$-bonds is reactive to isocyanate even under more drastic conditions for $Cp_2ZrR_2$ (R = Me, Ph, $CH_2Ph$),[16] $MoO_2(Mes)_2$,[21] $[Mn(CH_2Bu^t)_2]_4$,[5b] and $[Mn(CH_2CMe_2Ph)_2]_2$.[5b] In the latter case the steric factors were proposed to mitigate against coordination of a second organic isocyanate molecule, thus preventing its insertion. The insertion of a second PhNCO molecule into the Ln−C $\sigma$-bond may be attributed to two favorable facts: (i) the presence of a vacant coordination site at the bigger lanthanide metal center satisfies the need of precoordination of the PhNCO molecule preceding insertion; (ii) the stronger ionic characteristics of the Ln−C $\sigma$-bond enhance the migratory aptitude of the alkyl ligands. Consistent with the scenario that substrate precoordination must occur to access the intermediate is the fact that a large excess of PhNCO cannot be catalyzed to polymerize by the above transition-metal complexes.[5b,6]

Complexes **6** and **7** have been characterized by standard spectroscopic and analytical techniques. Complexes **6** and **7** have MS and IR spectra consistent with their known or assumed structure. Complex **7** has been structurally characterized by an X-ray analysis.

Table 4 lists the selected bond distances and bond angles in **7**. As depicted in Figure 4, the structure of **7** is well comparable to that of **1**. The holmium molecule resides on a crystallographic axis of 2-fold symmetry. The two bridging $PhNC(Bu^n)O$ ligands point in opposite directions, and the two metal atoms are equivalent. Each holmium ion is coordinated by two $\eta^5$-Cp′ groups, one chelating amido ligand, and one bridging O atom of a second amido ligand. Bond lengths and angles in the amido functions indicate also their bonding in an $\mu$-$\eta^1$:$\eta^3$-fashion. The bridging $Ho_2O_2$ unit is planar. The coordination number of the holmium atom is 10. The methylcyclopentadienyl groups on each holmium center are arranged in an eclipsed conformation. The complex has no unusual distances or angles in the $Cp'_2Ho$ unit. The average Ho−C(ring) distance of 2.647(4) Å is in the

**Table 4. Selected Bond Lengths (Å) and Angles (deg) in 7[a]**

| Bond Distances | | | |
|---|---|---|---|
| Ho(1)−O(1) | 2.442(3) | Ho(1)−N(1) | 2.437(3) |
| Ho(1)−O(1A) | 2.308(3) | Ho(1)−C(31) | 2.884(4) |
| Ho(1)−C(22) | 2.633(4) | Ho(1)−C(12) | 2.634(5) |
| Ho(1)−C(23) | 2.636(4) | Ho(1)−C(13) | 2.638(4) |
| Ho(1)−C(11) | 2.642(4) | Ho(1)−C(14) | 2.658(4) |
| Ho(1)−C(24) | 2.663(5) | Ho(1)−C(15) | 2.683(4) |
| Ho(1)−C(21) | 2.684(5) | Ho(1)−C(25) | 2.714 (5) |
| O(1)−C(31) | 1.319(5) | N(1)−C(31) | 1.286(5) |
| N(1)−C(1) | 1.430(5) | C(31)−C(32) | 1.506(5) |

| Bond Angles | | | |
|---|---|---|---|
| O(1A)−Ho(1)−N(1) | 119.2(1) | O(1)−Ho(1)−O(1A) | 67.4(1) |
| N(1)−Ho(1)−O(1) | 53.3(1) | Ho(1)−O(1)−Ho(1A) | 112.6(1) |
| C(31)−O(1)−Ho(1) | 95.5(2) | C(31)−O(1)−Ho(1A) | 149.7(3) |
| O(1)−C(31)−N(1) | 114.3(3) | C(31)−N(1)−C(1) | 123.5(3) |
| N(1)−C(31)−C(32) | 128.0(4) | O(1)−C(31)−C(32) | 117.5(4) |

[a] Symmetry transformation (A): $-x, 1-y, -z$.

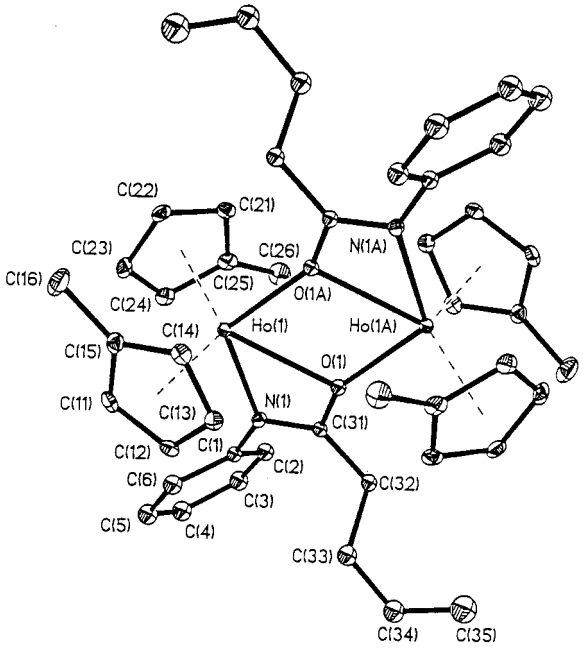


**Figure 4.** ORTEP diagram of $[Cp'_2HoOC(Bu^n)NPh]_2$ (**7**) with the probability ellipsoids drawn at the 30% level.

normal range.[22,23] The average Ho−O distance of 2.375(3) Å is longer than the values observed in $[(MeOCH_2CH_2C_5H_4)_2Ho(\mu\text{-}OH)]_2$ [2.250(3) Å][24] and $[(C_5H_5)Ho(PzMe_2)(OSiMe_2PzMe_2)]_2$ [2.280(4) Å].[23] The rather long Ho−O distance in **7** may be attributed to the facts that the oxygen atom is part of a delocalization chelating ligand system and that the larger steric crowding resulted from a higher coordination number. The O(1)−Ho−O(1A) angle of 67.4(1)° is slightly less than typical O−Ln−O angles in other dinuclear oxygen-bridge complexes.[13,23]

## Conclusions

The present results demonstrate that organolanthanide alkyl (aryl) complexes exhibit higher activity to phenyl isocyanate than some transition metal dialkyls.[5b,16,21] Not only can the phenyl isocyanate be inserted into each of the Ln−C $\sigma$-bonds of $Cp'_2LnR(THF)$ and $Cp'LnR_2(THF)_n$ under more mild conditions, but also the reaction is less affected by the properties of the R ligand. Moreover, in contrast to the trends of the sterically encumbered compound $Cp^*_3Sm$, where a second equivalent of substrate can be incorporated into the first insertion product, in the present case, the monoinsertion product catalyzed the excess of PhNCO to form the cyclotrimer. All observed differences indicate that the nature of the M−R bond and the steric crowding around the central metal ion may have a much greater influence on the insertion. Moreover, the X-ray analyses have revealed an unusual bonding mode of the amido groups arising from insertion of PhNCO into the Ln−C $\sigma$-bonds and that the O···C···N fragment of the $OC(Bu^n)NPh$ ligand acts as both a bridging and side-on chelating group.

## Experimental Section

**Materials and Methods.** All manipulations were carried out under argon with rigorous exclusion of air and moisture using Schlenk, vacuum-line, and glovebox techniques. All solvents were refluxed and distilled over sodium benzophenone ketyl immediately before use. $Cp'HoCl_2(THF)_3$,[25] $Cp'_2LnCl$ (Ln = Sm, Dy, Er, Yb; $Cp' = C_5H_4CH_3$),[26] and $Cp'_2Ln(Bu^n)$[4a] were prepared by the literature procedures. The phenyl isocyanate (Aldrich), α-bromonaphthalene (Fluka) and *n*-butyllithium (Fluka) were used without further purification. Elemental analyses for carbon, hydrogen and nitrogen were performed on a Rapid CHN-O analyzer. Metal analyses for lanthanides were accomplished using the literature method.[27] Infrared spectra were obtained on a NICOLET FT-IR 360 spectrometer with samples prepared as Nujol mulls. Mass spectra were recorded on a Philips HP5989A instrument operating in EI mode. Crystal samples of the respective complexes were rapidly introduced by the direct inlet techniques with a source temperature of 200 °C. The values of *m*/*z* are referred to the isotopes $^{12}C$, $^{1}H$, $^{14}N$, $^{152}Sm$, $^{164}Dy$, $^{165}Ho$, and $^{166}Er$.

**$[Cp'_2SmOC(Bu^n)NPh]_2$ (1).** To a solution of $Cp'_2SmCl$(THF) (0.302 g, 0.725 mmol) in THF (30 mL) was added *n*-butyllithium (1.24 M, in cyclohexane, 0.58 mL) at −30 °C. After stirring for 4 h, to the mixture was added phenyl isocyanate (0.08 mL, 0.725 mmol) at −10 °C. The reaction mixture was then warmed to ambient temperature and stirred overnight. The solvent was removed by reduced pressure. The solid was extracted with toluene. The resulting yellow solution was concentrated by reduced pressure to about 5 mL, and a yellow solid precipitated. The precipitate was resolved by addition of 2 mL of THF. Yellow crystals of **1** (0.26 g, 74%) were obtained upon cooling at −30 °C, mp 174 °C. Anal. Calcd for $C_{46}H_{56}N_2O_2Sm_2$: C, 56.98; H, 5.82; N, 2.89; Sm, 31.01. Found: C, 56.76; H, 5.73; N, 2.90; Sm, 30.67. IR (KBr pellet, $cm^{-1}$): 1664 m, 1568 m, 1556 m, 1463 s, 1377 s, 1330 m, 1277 w, 1232 w, 1093 w, 1045 w, 1026 m, 1012 m, 955 m, 820 m, 778 s, 754 s, 723 s, 699 m, 656 w, 619 w. MS: *m*/*e* [fragment, relative intensity %] = 893 [M − Cp′, 3], 814 [M − 2Cp′, 1], 716 [M − $OC(Bu^n)NPh$-Cp′H, 1], 486 [M/2, 2], 429 [M/2 − $C_3H_6$, 40], 407 [M/2 − Cp′, 100], 328 [M/2 − 2Cp′, 44], 310 [$Cp'_2Sm$, 21], 231 [Cp′Sm, 24], 79 [Cp′, 20], 77 [Ph, 40], 57 [$Bu^n$, 4].

**$[Cp'_2DyOC(Bu^n)NPh]_2$ (2).** To a solution of $Cp'_2DyCl$ (0.196 g, 0.55 mmol) in THF (30 mL) was added *n*-butyllithium (1.28 M, in cyclohexane, 0.43 mL) at −30 °C. After stirring for 4 h,

(24) Deng, D. L.; Jiang, Y. Q.; Qian, C. T.; Wu, G.; Zheng, P. J. *J. Organomet. Chem.* **1994**, *470*, 99.

(25) Zhou, X. G.; Huang, Z. E.; Cai, R. F.; Xie, M. H.; You, X. Z.; Xu, Z. *Chin. J. Inorg. Chem.* **1998**, *14*, 68.

(26) Maginn, R. E.; Manastyrskj, S.; Dubeck, M. *J. Am. Chem. Soc.* **1963**, *85*, 672.

(27) Qian, C. T.; Ye, C. Q.; Lu, H. Z.; Li, Y. Q.; Zhou, J. L.; Ge, Y. W. *J. Organomet. Chem.* **1983**, *247*, 161.

to the mixture was added phenyl isocyanate (0.06 mL, 0.55 mmol) at −15 °C. The reaction mixture was subsequently worked up by the method described above. Yellow crystals of **2** were obtained in 54% yield. Anal. Calcd for $C_{46}H_{56}N_2O_2Dy_2$: C, 55.58; H, 5.68; N, 2.82; Dy, 32.70. Found: C, 55.17; H, 5.64; N, 2.86; Dy, 32.31. IR (KBr pellet, $cm^{-1}$): 2729 m, 2671 m, 1670 w, 1600 w, 1571 m, 1554 w, 1462 s, 1377 s, 1304 m, 1155 w, 1074 m, 1028 w, 1009 w, 964 w, 821 w, 774 m, 754 m, 727 s, 694 m, 658 w, 590 m. MS: *m/e* [fragment, relative intensity %] = 917 [M − Cp′, 100], 838 [M − 2Cp′, 3], 498 [M/2, 15], 419 [M/2 − Cp′, 13], 340 [M/2 − 2Cp′, 8], 322 [$Cp'_2Dy$, 15], 79 [Cp′, 23], 77 [Ph, 17].

**[$Cp'_2ErOC(Bu^n)NPh]_2$ (3).** Following the procedure described for **1**, reaction of $Cp'_2ErCl$ (0.321 g, 0.89 mmol) with *n*-butyllithium (1.15 M, 0.77 mL) and subsequently with PhNCO (0.097 mL, 0.89 mmol) gave **3** as pink crystals. Yield: 0.277 g (62%). Anal. Calcd for $C_{46}H_{56}N_2O_2Er_2$: C, 55.07; H, 5.62; N, 2.79; Er, 33.34. Found: C, 55.13; H, 5.66; N, 2.82; Er, 33.42. IR (KBr pellet, $cm^{-1}$): 1604 m, 1571 m, 1463 s, 1377 s, 1341 m, 1240 w, 1071 w, 1031 w, 1012 m, 964 m, 827 m, 772 s, 754 s, 723 s, 702 m, 670 w, 619 w. MS: *m/e* [fragment, relative intensity %] = 921 [M − Cp′, 100], 842 [M − 2Cp′, 2], 500 [M/2, 17], 421 [M/2 − Cp′, 21], 342 [M/2 − 2Cp′, 3], 324 [$Cp'_2Er$, 6], 245 [Cp′Er, 3], 79 [Cp′, 13].

**[$Cp'_2DyOC(Np)NPh]_2$ (4).** To a stirred THF solution (10 mL) of *n*-butyllithium (1.68 mmol) at −15 °C was added dropwise α-bromonaphthalene(NpBr) (0.23 mL, 1.68 mmol). After stirring for 30 min, the reaction solution was allowed to warm to room temperature and stirred for a further 30 min. Then, the reaction solution was added to a solution of $Cp'_2DyCl$ (0.598 g, 1.68 mmol) in THF (25 mL) at −15 °C, and the mixture was stirred at room temperature for 4 h. Phenyl isocyanate (0.18 mL, 1.68 mmol) was added at −30 °C. The reaction was stirred overnight. The solvent was removed in vacuo. The residue solid was extracted with toluene. Recrystallization by vapor diffusion of hexane into a toluene solution afforded pale yellow crystals of **4**·THF. Yield: 0.50 g (52%). Anal. Calcd for $C_{62}H_{60}N_2O_3Dy_2$: C, 61.74; H, 5.01; N, 2.32; Dy, 26.95. Found: C, 61.24; H, 4.98; N, 2.32; Dy, 27.03. IR (KBr pellet, $cm^{-1}$): 3057 w, 1640 w, 1588 m, 1568 s, 1530 w, 1500 w, 1400 m, 1351 s, 1250 w, 1207 m, 1143 m, 1075 w, 1068 w, 1.035 m, 1013 m, 925 m, 870 w, 838 m, 776 s, 732 m, 702 s, 595 w, 558 m. MS: *m/e* [fragment, relative intensity %] = 567 [M/2 − 1, 11], 553 [M/2 − $CH_3$, 3], 488 [M/2 − Cp′H, 48], 410 [M/2 − 2Cp′, 1], 241 [Cp′Dy, 11], 127 [Np, 7], 91 [NPh, 100], 79 [Cp′, 9], 72 [THF, 1].

**General Procedure for Catalytic Formation of $[PhNCO]_3$ (5). Method A.** A mixture of PhNCO (0.40 mmol), $[Cp'_2DyOC(Bu^n)NPh]_2$ (0.20 mmol), and THF (15 mL) was magnetically stirred at 0 °C for 8 h. The color of the solution changed slowly from pale yellow to orange. After stirring for a further 12 h at room temperature, the solvent was removed by vacuum, and the resulting solid was extracted with toluene. Crystallization from toluene/hexane afforded **5**·THF as pale yellow crystals. Yield: 0.03 g (52%), mp 278 °C. Anal. Calcd for $C_{25}H_{23}N_3O_4$: C, 69.91; H, 5.40; N, 9.78. Found: C, 69.72; H, 5.28; N, 9.91. IR (KBr pellet, $cm^{-1}$): 3065 w, 1706 s, 1590 m, 1488 s, 1455 s, 1414 s, 1290 m, 1219 m, 1157 w, 1074 s, 1028 m, 918 m, 814 m, 752 s, 690 s, 590 s. MS: *m/e* [fragment, relative intensity %] = 357 [M, 100], 238 [M − PhNCO, 6], 119 [PhNCO, 94], 77 [Ph, 8]. **5** was also obtained (55% yield) from the higher molar ratio of PhNCO to **2** (10:1).

**Method B.** To 20 mL THF solution of $Cp'_2DyBu^n$ (0.525 mmol) at −20 °C was added an excess of phenyl isocyanate (1.82 mmol), and the solution was stirred overnight. After warming to room temperature and stirring for 3 h the reaction was quenched with water and extracted with toluene. The organic portions were combined and washed with water. The solvent was removed in vacuo. Yellow crystals were obtained by recrystallization in toluene/hexane. Yield: 0.132 g (61%). The physical, analytical, and spectroscopic properties of the compound were identical with that obtained above.

**$Ho[OC(Bu^n)NPh]_3$ (6).** To a solution of $Cp'HoCl_2(THF)_3$ (0.530 g, 1.00 mmol) in 45 mL of THF was added butyllithium (1.15 M, 1.74 mL) at −30 °C. After stirring at this temperature for 3 h, the solution was allowed to warm to 0 °C, where it was stirred for 1.5 h. Then, the solution was cooled to −30 °C and treated with 0.22 mL (2.0 mmol) of PhNCO. After stirring for 3 h at −30 °C, the reaction mixture was slowly warmed to ambient temperature and was stirred for 48 h. Removal of solvent left yellow solids. The resulting solid was extracted with cold toluene. The extract was evaporated to ca. 5 mL. A yellow microcrystalline solid was slowly formed at 30 °C, which disappeared at −15 °C. Yield: 0.22 g (63%). Anal. Calcd for $C_{33}H_{42}O_3N_3Ho$: C, 57.14; H, 6.10; N, 6.05; Ho, 23.78. Found: C, 56.67; H, 6.05; N, 6.09; Ho, 23.85. IR (KBr pellet, $cm^{-1}$): 1659 w, 1631 m, 1298 m, 774 w, 481 s.

**$[Cp'_2HoOC(Bu^n)NPh]_2$ (7).** Further crystallization by diffusion of hexane into the above mother liquor yielded yellow crystals of **7**, which were collected, washed with a minimal amount of the mixture solution of THF and hexane, and dried in a vacuum. Yield: 0.160 g (64%). Anal. Calcd for $C_{46}H_{56}N_2O_2Ho_2$: C, 55.31; H, 5.65; N, 2.80; Ho, 33.03. Found: C, 55.43; H, 5.66; N, 2.92; Ho, 33.42. MS: *m/e* [fragment, relative intensity %] = 919 [M − Cp′, 100], 863 [M − Cp′-$Bu^n$H, 3], 840 [M − 2Cp′, 1], 822 [M − OC($Bu^n$)NPh, 8], 742 [M − OC-($Bu^n$)NPh-Cp′H, 2], 680 [M − 4Cp′-2, 2], 499 [M/2, 12], 457 [M/2 − $C_3H_6$, 4], 420 [M/2 − Cp′, 12], 323 [$Cp'_2Ho$, 4], 79 [Cp′, 2], 77 [Ph, 7], 57 [$Bu^n$, 1].

**Structure Determination.** Suitable single crystals of complexes **1**, **4**·THF, **5**·THF, and **7** were sealed in thin-walled glass capillaries under argon for the X-ray diffraction study. Crystal data and details of collection and refinement are summarized in Table 5.

**For 1**, diffraction experiments were performed on a Bruker SMART 1000 CCD diffractometer ($\lambda = 0.71069$ Å, $\omega-2\theta$ scans). Frames were integrated to a maximum $2\theta$ angle of 52.76° with the Siemens SAINT program to yield a total of 4875 reflections, of which 4157 were independent ($R_{int} = 0.0188$) and 3900 were above $2\sigma(I)$. Laue symmetry revealed a triclinic crystal system, and the final unit cell parameters were determined from the least-squares refinement of three-dimensional centroids of 5102 reflections. Data were corrected for absorption with the SADABS program.[28] The structure was solved by direct methods, expanded using Fourier technique, and refined on $F^2$ by full-matrix least-squares.[29] All non-hydrogen atoms were refined anisotropically, and all hydrogen atoms were included in idealized positions with isotropic thermal parameters related to those of the supporting carbon atoms, but were not included in refinement. All calculations were performed by using the SHELXS-97 crystallographic software package.[30]

**For 4**·THF, preliminary examination and intensity data collection were carried out with an Enraf-Nonius CAD-automatic diffractometer using graphite-monochromatized Mo Kα radiation. Accurate cell paramaters were obtained by the least-squares refinement of the setting angles of 25 reflections with $11.06° < \theta < 12.62°$. Intensity data were collected using the $\omega-2\theta$ scan mode and corrected for absorption and decay. The structures were solved by direct methods and refined with full-matrix least-squares on $F^2$. The solvent molecule THF was disordered, and no "model" could be proposed to "fit" THF to the observed electron density maps, so bond distances were constrained.

**For 5**·THF, the X-ray intensity data were collected as for **1** above. Frames were integrated to a maximum $2\theta$ angle of

(28) Sheldrick, G. M. *SADABS, A Program for Empirical Absorption Correction*; Göttingen, Germany, 1998.

(29) *SHLXTL PLUS*, Siemens Analytical X-ray Institute Inc., XS: Program for Crystal Structure Solution, XL: Program for Crystal Structure Determination, XP: Interactive Molecular Graphics, 1990.

(30) Sheldrick, G. M. *SHELXL-97*, Program for the refinement of the crystal structure; University of Göttingen: Germany, 1997.

**Table 5. Crystal and Data Collection Parameters of Complexes 1, 4·THF, 5·THF, and 7**

| | **1** | **4**·THF | **5**·THF | **7** |
|---|---|---|---|---|
| formula | $Sm_2C_{46}H_{56}N_2O_2$ | $Dy_2C_{62}H_{60}O_3N_2$ | $C_{25}H_{23}N_3O_4$ | $Ho_2C_{46}H_{56}O_2N_2$ |
| molecular weight | 969.62 | 1206.12 | 429.46 | 998.79 |
| cryst color, shape | yellow | yellow | pale yellow | yellow |
| cryst dimens (mm) | 0.50 × 0.40 × 0.30 | 0.68 × 0.20 × 0.20 | 0.35 × 0.25 × 0.20 | 0.80 × 0.50 × 0.30 |
| cryst syst | triclinic | orthorhombic | triclinic | monoclinic |
| space group | $P\bar{1}$ | $Fdd2$ | $P\bar{1}$ | $P2_1/n$ |
| lattice params | | | | |
| $a$ (Å) | 9.2183(7) | 15.815(3) | 11.2424(8) | 13.494(3) |
| $b$ (Å) | 11.1378(9) | 23.014(5) | 11.3102(9) | 8.8476(18) |
| $c$ (Å) | 11.4694(9) | 28.168(6) | 11.4925(9) | 17.708(4) |
| α (deg) | 111.920(1) | 90.00 | 91.145(2) | 90.00 |
| $\beta$ (deg) | 103.173(1) | 90.00 | 115.072(1) | 98.40(3) |
| $\gamma$ (deg) | 97.794(1) | 90.00 | 115.093(1) | 90.00 |
| $V$ (Å$^3$) | 1031.5(1) | 10252(4) | 1108.5(2) | 2091.4(7) |
| $Z$ | 1 | 8 | 2 | 2 |
| $D_c$ (g cm$^{-3}$) | 1.535 | 1.563 | 1.287 | 1.586 |
| $F$(000) | 470 | 4816 | 452 | 992 |
| radiation ($\lambda$ = 0.71069 Å) | Mo Kα | Mo Kα | Mo Kα | Mo Kα |
| temp (K) | 298(2) | 293(2) | 298(2) | 293(2) |
| scan type | $\omega-2\theta$ | $\omega-2\theta$ | $\omega-2\theta$ | $\omega-2\theta$ |
| $\mu$ (mm$^{-1}$) | 2.856 | 2.941 | 0.089 | 3.793 |
| $hkl$ range | −11−11, −13−11, −14−14 | −19−16, −16−28, −34−0 | −7−13, −13−13, −13−13 | 0−16, 0−10, −21−21 |
| $\theta$ range (deg) | 2.01−26.38 | 1.72−26.00 | 2.04−25.02 | 1.78−26.02 |
| no. of reflns measd | 4875 | 5174 | 4653 | 3993 |
| no. of unique reflns | 4157 ($R_{int}$ = 0.0188) | 2566 ($R_{int}$ = 0.1543) | 3900 ($R_{int}$ = 0.0162) | 3831 ($R_{int}$ = 0.0353) |
| no. of reflns obsd | 3900[$I > 2\sigma(I)$] | 1653[$I > 2\sigma(I)$] | 3250 | 3499[$I > 2\sigma(I)$] |
| refinement method | full-matrix least-squares on $F^2$ | | | |
| no. of variables | 238 | 144 | 370 | 235 |
| $w$ | $1/[\sigma^2(F_o^2) + (0.064P)^2 + 0.9171P]$ with $P = (F_o^2 + 2F_c^2)/3$ | $1/[\sigma^2(F_o^2) + (0.0884P)^2 + 0.0000P]$ with $P = (F_o^2 + 2F_c^2)/3$ | $1/[\sigma^2(F_o^2) + (0.0808P)^2 + 0.1972P]$ with $P = (F_o^2 + 2F_c^2)/3$ | $1/[\sigma^2(F_o^2) + (0.0557P)^2 + 0.3917P]$ with $P = (F_o^2 + 2F_c^2)/3$ |
| goodness of fit on $F^2$ | 1.057 | 0.967 | 1.021 | 1.158 |
| final $R$ indices [$I > 2\sigma(I)$] | $R_1$ = 0.0324 | $R_1$ = 0.0692 | $R_1$ = 0.0443 | $R_1$ = 0.0258 |
| | $wR_2$ = 0.0866 | $wR_2$ = 0.1643 | $wR_2$ = 0.1271 | $wR_2$ = 0.0833 |
| $R$ indices (all data) | $R_1$ = 0.0345 | $R_1$ = 0.1148 | $R_1$ = 0.0521 | $R_1$ = 0.0300 |
| | $wR_2$ = 0.0891 | $wR_2$ = 0.1875 | $wR_2$ = 0.1370 | $wR_2$ = 0.0845 |
| largest diff peak and hole (e Å$^{-3}$) | 1.223, −1.191 | 1.400, −2.138 | 0.260, −0.153 | 0.784, −0.824 |

52.78° with the Siemens SAINT program to yield a total of 3883 reflections, of which 3274 were independent ($R_{int}$ = 0.0181) and 3105 were above $2\sigma(I)$. Laue symmetry revealed a triclinic crystal system, and the final unit cell parameters were determined from the least-squares refinement of three-dimensional centroids of 3665 reflections. A total of 3274 independent reflections were collected in the range 2.84° < $\theta$ < 25.02° by using the $\omega-2\theta$ scan mode at 298(2) K; 3105 observable reflections with $I > 2\sigma(I)$ were used in the succeeding refinements. The intensities were corrected for Lorentz−polarization effects and empirical absorption with the SADABS program. The structure was solved by direct methods using the SHELXL-97 program. Refinement on $F^2$ was performed by full-matrix least-squares with anisotropic thermal parameters for all non-hydrogen atoms. There is one tetrahydrofuran molecule present per formula unit. All calculations were performed using the Bruker Smart program.

**For 7**, the X-ray intensity data were collected on a Rigaku AFC5R diffractometer. Final cell parameters were based on a least-squares analysis of 20 reflections in well-separated regions of reciprocal space, all having 7.61° < $\theta$ < 9.87°. All 3831 unique data were corrected for the effects of absorption and for Lorentz and polarization factors. The structure was solved by direct methods with the program SHELXTL.[31] In the final cycles, all non-hydrogen atoms were refined anisotropically and all hydrogen atoms were fixed at idealized positions.

**Acknowledgment.** We thank the National Natural Science Foundation of China and the Research Fund for the Doctoral Program of Higher Education of China and the Shuguang Foundation of Shangai Education Committee of China for financial support.

**Supporting Information Available:** Tables of atomic coordinates and thermal parameters, all bond distances and angles, and experimental data for all structurally characterized complexes. This material is available free of charge via the Internet at http://pubs.acs.org.

OM010346Y

(31) Sheldrick, G. M. *SHELXTL*, Structure Analysis Program; Siemens Industrial Automation Inc.: Madison, WI, 1994.